LEGIBILITY NOTICE

A major purpose of the Technical Information Center is to provide the broadest dissemination possible of information contained in DOE's Research and Development Reports to business, industry, the academic community, and federal, state and local governments.

Although a small portion of this report is not reproducible, it is being made available to expedite the availability of information on the research discussed herein.

Los Alamos National Laboratory is operated by the University of California for the United States Department of Energy under contract W-7405-ENG-36

LA-UR--89-1649

DE89 013454

TITLE PARTICLE PRODUCTION RESULTS FROM HELIOS

AUTHOR(S) Barbara Jacak, P-2

SUBMITTED TO 3rd Conference on the Intersections Between Particle and Nuclear Physics, Rockport, Maine, May 14-19, 1988

DISCLAIMER

MASTER

Los Alamos Los Alamos National Laboratory
Los Alamos, New Mexico 87545

PARTICLE PRODUCTION RESULTS FROM HELIOS

Barbara Jacak
Los Alamos National Laboratory, Los Alamos NM, 87545

THE HELIOS COLLABORATION

The availability of ultrarelativistic heavy ion beams at CERN and Brookhaven allows investigation of the physical properties of a state of high energy density in nuclear matter. The interest is driven by the expectation that confinement of the partons in a hadron cannot survive when the density of hadrons is large compared to the density inside ordinary hadrons. This prospect is supported by QCD calculations[1], and collisions between heavy nuclei at ultrarelativistic energies are predicted to provide the energy densities required for deconfinement (greater than 2-3 GeV/fm^3). Among the goals of the first experiments are investigation of the energy density and spatial extent of the highly excited central rapidity region to address whether the necessary conditions have been satisfied, and a closer examination of events with large amounts of energy deposited in the target. The HELIOS (High Energy Lepton and Ion Spectrometer) experiment therefore combines 4 π calorimetric coverage with measurement of charged particle multiplicity, inclusive particle spectra, two particle correlations, lepton pairs and photons.

The target region is surrounded by a box of calorimeter modules that cover the pseudorapidity interval $-0.1 < \eta < 2.9$. The forward region is covered by a beam calorimeter placed further downstream. The granularity of this calorimeter allows extension of the E_t measurement to $\eta = 4.9$. The transverse energy cross-sections $d\sigma/dE_t$ are presented in Figure 1 for ^{16}O beams at 60 and 200 GeV per nucleon incident on W, Ag and Al targets[2]. The main feature of the distributions is a long plateau followed by a steeply falling tail, reflecting the shape of the overlap integral of nuclear densities in collisions with random impact parameters[3]. The large value of E_t attained is striking. At 200 GeV/A, values of 200 GeV are reached; adding the E_t measured for $\eta > 2.9$ increases this to 280 GeV. This is ~0.73 of the value of the kinematic limit, and shows that nuclei are not transparent to one another at these beam energies. An important result of the first experiments is that the calculated energy density is still increasing at 200 GeV/A.

The curves in fig. 1 are fits to the geometrical overlap integral, folded with a Gaussian distribution in E_t per N-N collision[3]. This procedure yields an excellent description of the data, with the fitted mean of approximately 1 GeV, which may be compared with the mean E_t of ~ 1.4 GeV in p-p collisions at $\sqrt{s}$ = 20 GeV.

Figure 2 shows the transverse energy distributions measured for ^{16}O and ^{32}S beams at 200 GeV/A, incident on a W target. The maximum transverse energy achieved with the S beam is approximately twice that of the O beam, suggesting that the energy density stays approximately constant while the "thermalized" volume increases. The bands depict predictions made with IRIS, an event generator incorporating the collision geometry with the dual parton model[4]. The width of the

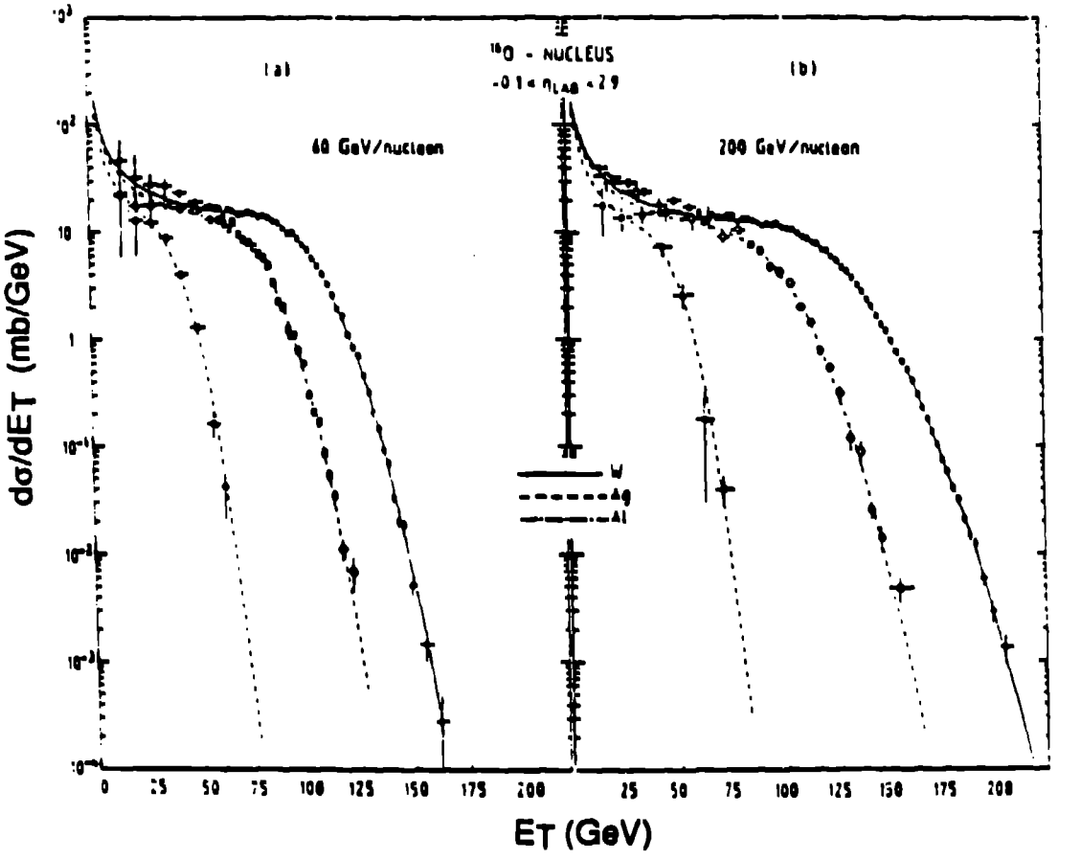

FIGURE 1
The transverse energy distributions measured at a) 60 GeV per nucleon, b) 200 GeV per nucleon. The curves are fits to the geometrical overlap integral, folded with a Gaussian distribution in E_t per N-N collision [2].

bands represents the effect of the absolute E_t scale uncertainty. IRIS is seen to underpredict the transverse energy for both beams. Such a result is not surprising as the calculation does not account for cascading of secondary particles in the target.

In parallel with the E_t measurements, the charged particle multi- plicities have been measured with silicon detectors. These detectors have approximately 400 segments each, and are positioned 3 and 9 cm downstream from the target. The multiplicity distribution exhibits a similar plateau and tail to the E_t distributions, and the multiplicity is seen to increase linearly with Et. One can infer from p-p collisions and HIJET, together with the known calorimeter response, that 55% of the E_t is produced by charged particles. This allows one to estimate an average pt per particle of ~ 340 MeV/c. Though this may increase very slightly with E_t, we conclude that high transverse energies arise via formation of many charged particles, rather than by a large change in the momentum distributions of the particles.

Figure 3 shows the pseudorapidity distributions of both E_t and charged particle multiplicity for central collisions of 200 GeV/A O + W. Though the comparison is limited by the calorimeter granularity, the two distributions agree rather well. They show a broad peak with maximum density between $\eta = 2$ and 2.5, clearly shifted backward from the p-p center of mass, $\eta \sim 3$. The values are close to $\eta = 2.4$, the center of mass rapidity characteristic of a system of 16 projectile nucleons stopped by 50 nucleons from the target. Also in figure 3 are the $dE_t/d\eta$ predictions from IRIS. The calculation is clearly more forward peaked than the data, and the rapidity densities in the backward region are underpredicted. These effects are both consistent with expectations from target cascading.

From the E_t and multiplicity measurements we have learned that there are no drastic changes in the nature of the charged particles emitted; larger E_t is the result of more charged particles. Nevertheless, a direct measurement is necessary to study the details of the charged particle momentum spectra. These may indicate the degree of thermalization reached in the collision, and allow a search for evidence of radial flow in the boost of heavy particle spectra. To aid in understanding the charged particle spectra, the transverse energy flow can be used to sort events according to impact parameter and energy deposition.

HELIOS measures charged particles with a magnetic spectrometer which views the target through a narrow slit in the calorimeter wall, covering the pseudorapidity interval $0.9 < \eta < 2.0$. A magnet with a p_t kick of ~ 80 MeV/c and two high resolution (175 μm) drift chambers provide the momentum measurement of charged particles. Particles are tracked back through the slit to the target to eliminate background from the calorimeters around the slit. Particle identification is achieved via time-of-flight and Aerogel Cerenkov counters.

Three data samples are presented: p + W, ^{16}O + W and ^{32}S + W, all at 200 GeV per nucleon. The data are triggered on the presence of a valid interaction and transverse energy observed in the calorimeters. Varying scale-down factors were used at the trigger level to ensure uniform statistical coverage over the entire E_t range. The measured pt spectra were corrected for various detector effects, namely geometrical acceptance, decays in flight, photon conversion in upstream material, reconstruction efficiency, and finite momentum resolution.

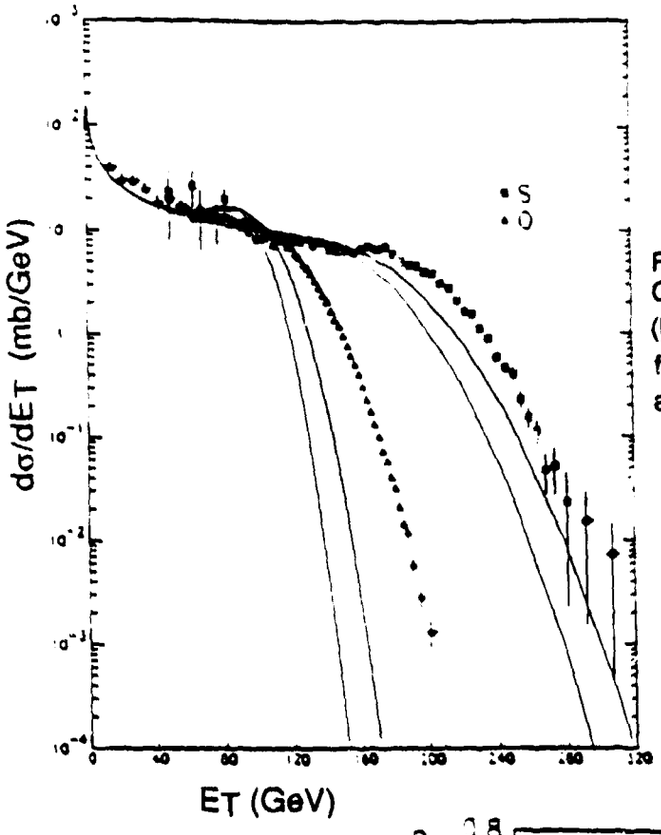

FIGURE 2
Comparison of IRIS predictions (band) with the data on dsig/dEt for O and S + W collisions at 200 GeV per nucleon.

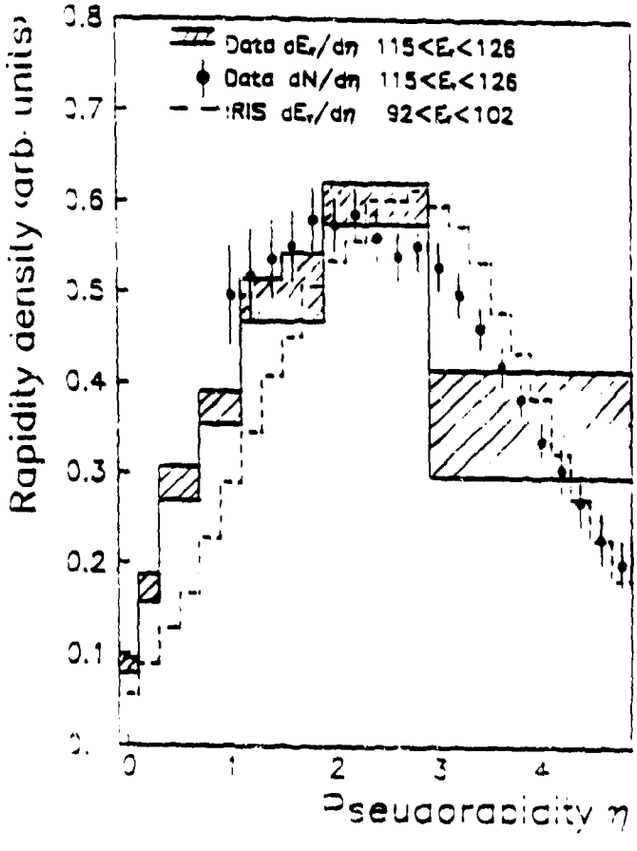

FIGURE 3
Comparison of the pseudorapidity distributions of transverse energy (solid lines), charged particle multiplicity (points), and IRIS prediction of $dE_T/deta$ (dotted line).

P_t spectra were simulated including all detector properties, and reconstructed using the full analysis chain: the ratio of input and reconstructed spectra is used to correct the data presented below. To generate the spectra we used a parameterization combining FNAL and CERN ISR measurements of charged particles, taking into account the c.m. energy dependence, the rapidity, and the well-known hardening of the p_t spectra in p+A collisions[5,6]. Systematic errors were estimated by comparing the corrected p_t spectra for nearby regions in pseudorapidity; in addition small variations of the detector response between the data sets were investigated. The systematic error is approximately 20%, but it should be noted that this yields an error in the slope of less than 3%.

Figure 4 shows the transverse momentum spectra for negative particles entering the spectrometer in p + W, O + W and S + W collisions at 200 GeV/A. The data are in the rapidity range $0.9 < y < 1.9$ (the transformation from pseudorapidity to rapidity neglects the small admixture of K^- in the negative particle spectrum) and the pt range $0.075 < p_t < 2.0$ GeV/c. The dashed line is the result of the parameterization described above. It is important to note that these data are taken from E_t triggered events, and are therefore biased toward central collisions.

All three data sets are well described by the parameterization, indicating that charged particles emitted in central nucleus-nucleus collisions show the same behavior as those from proton-nucleus collisions. S + W collisions yield a charged particle distribution identical to that from O + W collisions. The p_t spectra clearly cannot be described by a single exponential, and we have derived the inverse slopes in the regions $0.5 < p_t < 2.0$ GeV/c and $0.1 < p_t < 0.2$ GeV/c. The results are ~ 190 MeV/c and 85 MeV/c, respectively. The rise in cross section at low p_t has also been reported in heavy ion reactions in the streamer chamber at CERN[7] and in p - nucleus collisions at Fermilab 8. In all three experiments this could be a target fragmentation effect.

Figure 5 presents ratios of negative particle spectra for events in different regions of E_t, as a function of p_t. This plot allows careful comparison of the spectral shape over the entire p_t range. It is important to note that the ratios shown are normalized by the number of events in each spectrum; absolute normalizations may change these ratios from unity. All four curves are flat within statistical errors, and should be relatively insensitive to systematic errors. They indicate that the transverse momentum spectrum of charged particles does not change as the E_t of the collision increases. Note that this analysis probes the character of the charged particles from events in the tail of the E_t distribution. These have $E_t \geq 100$ MeV, and represent only about 10% of the total cross section, i.e. the most central collisions. The reference spectrum is taken from events with $55 < E_t < 100$ GeV, which lie in the plateau of the E_t distribution. Figure 1 and the geometrical description of the collision indicate that collisions included in figure 5 range from near overlap of the projectile and target to the smallest impact parameters. Thus we do not see the hardening of the p_t spectra at very high multiplicity (or E_t) that was predicted as a signature of deconfinement[9].

In order to study the charged particle spectra over the entire range of impact parameters, we calculate the mean p_t of the distribution over a limited range. This allows a detailed study of the variation of $\langle p_t \rangle$ with E_t. The $\langle p_t \rangle$ vs. E_t

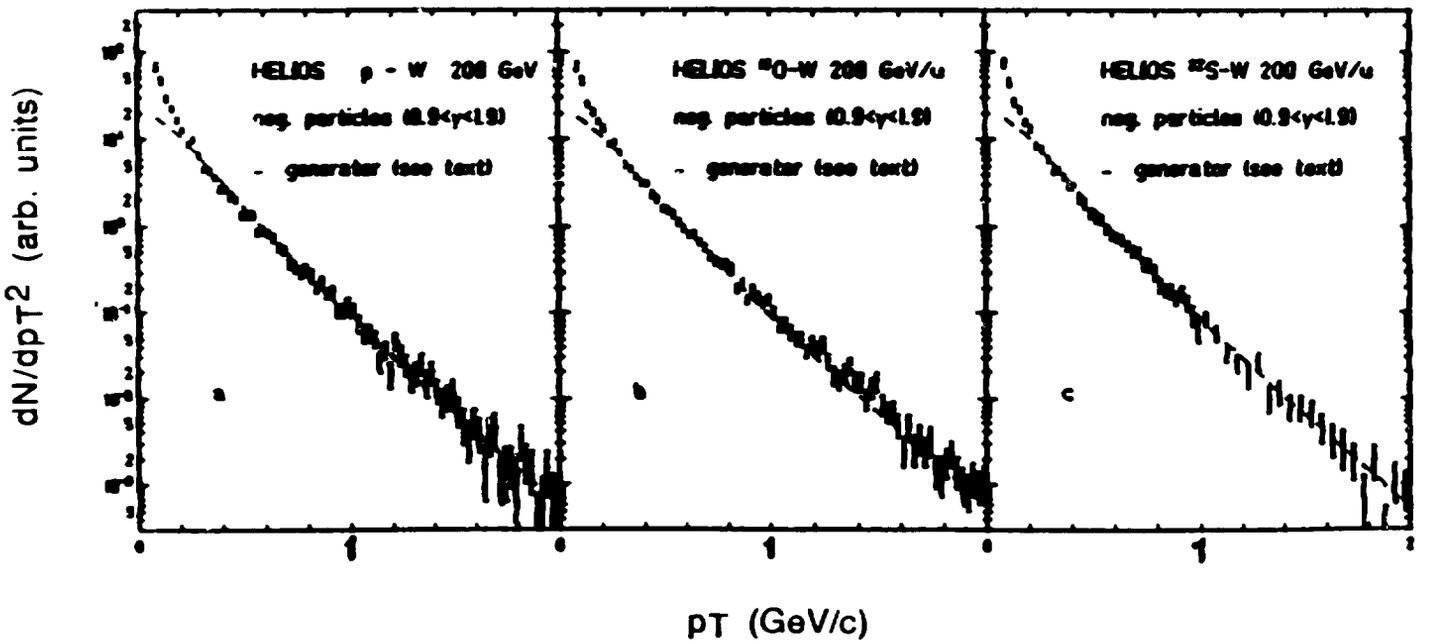

FIGURE 4
P_t spectra of negative particles detected in the external spectrometer for a) p + W, b) O + W, c) S + W at 200 GeV/A. The dashed line shows the results of a parameterization of p-p and p-A data described in the text.

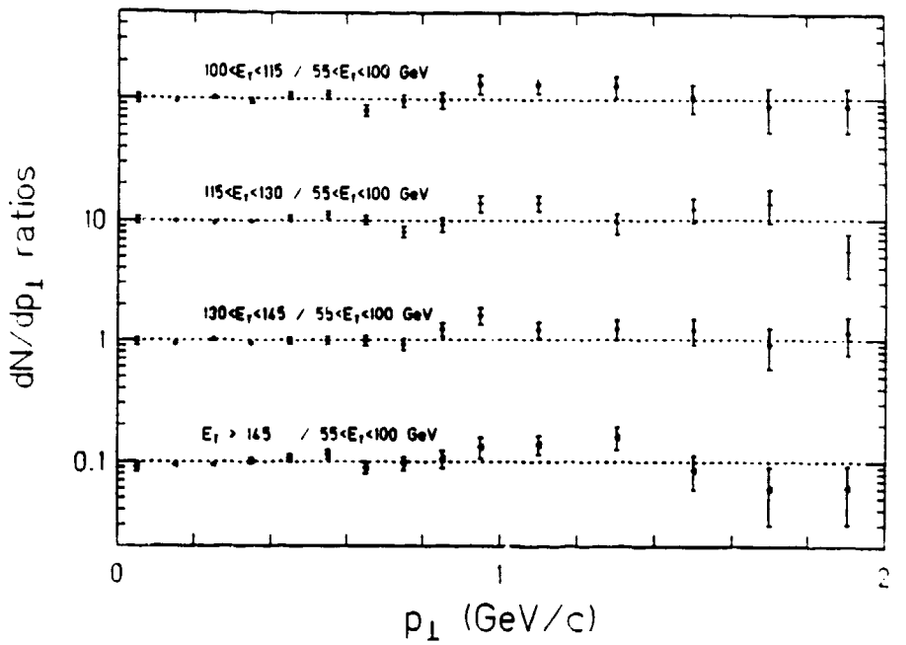

FIGURE 5
Ratios of negative particle spectra from O + W collisions at 200 GeV/A, plotted as a function of p_t. The ratios are normalized by the number of events in each spectrum. The four curves correspond to four regions of E_t, all normalized to the negative particle spectrum in events with 55 GeV < E_t < 100 GeV. The curves are offset by factors of 10 for clarity.

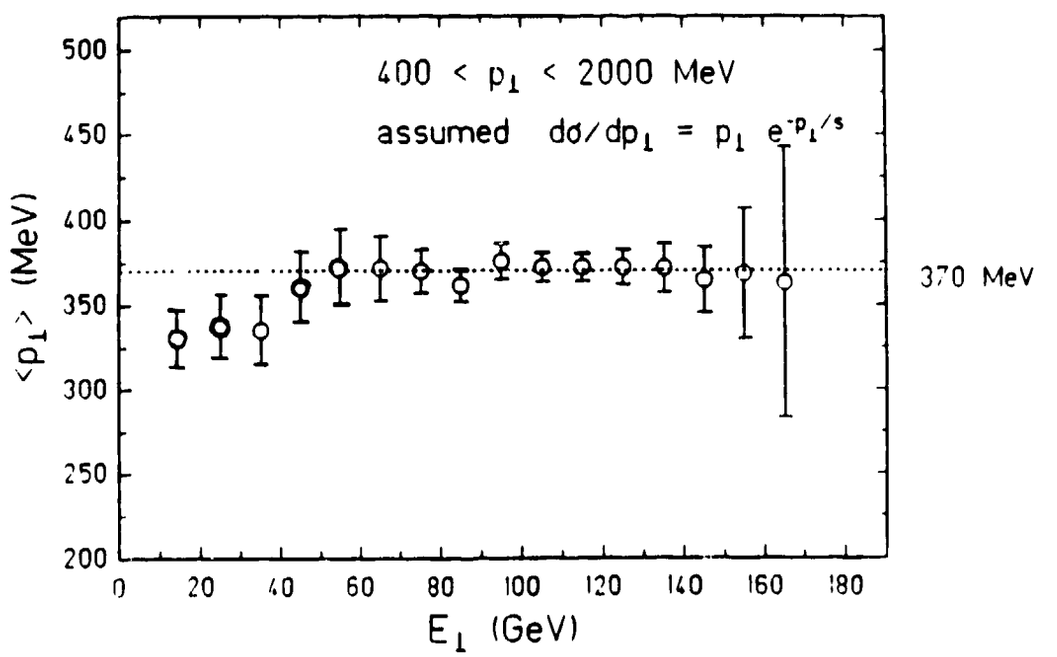

FIGURE 6
$\langle p_t \rangle$ as a function of E_t for 200 GeV/A O + W. The $\langle p_t \rangle$ is derived from the measured spectra by correcting the mean value in the range 0.4 < p_t < 2.0 GeV/c under the assumption of an exponential spectrum.

for negative particles from 200 GeV/A O + W is plotted in Figure 6. The values are calculated by determining mean pt in the range $0.4 < p_t < 2.0$ GeV/c and extrapolating to the mean of the entire spectrum under the assumption of a purely exponential shape. This method yields $\langle p_t \rangle$ which is not sensitive to the low p_t rise; the resulting values should be free of target effects and may be compared with p-p collisions. The $\langle p_t \rangle$ thus obtained can still, however, be affected by any deviations in the spectral shape away from exponential. Figure 4 shows that the spectra begin to follow a power law behavior above p_t of ~ 1.5 GeV/c, where one would expect to see effects of multiple hard scattering processes[6]. Thus the calculated $\langle p_t \rangle$ will be somewhat higher than from a slope fitted to the purely exponential part of the spectrum. Figure 6 shows that central collions, with $E_t >$ ~60 GeV, yield a constant $\langle p_t \rangle$ of 370 MeV/c. This should be compared with the IRIS prediction of 360 MeV/c for all charged particles and with 350 MeV/c for pions from p-p collisions[5]. For $E_t \leq 40$ GeV, corresponding to relatively peripheral collisions, $\langle p_t \rangle$ is lower, falling by ~ 40 MeV/c for the events with the lowest E_t. An increase in $\langle p_t \rangle$ with multiplicity or E_t of the collisions is predicted in models incoporating a hydrodynamical expansion of the highly excited central region[10]. However, the pt spectrum should also be strongly influenced by the hadronization process, making interpretation of the observe change more difficult.

In summary, we have seen that global variables such as transverse energy and multiplicity can be used to characterize events according to impact parameter. E_t and multiplicity show a linear relationship, indicating that higher E_t arises from production of more particles rather than a large change in the particle spectra. The shapes of the distributions can be explained by superposition of nucleon-nucleon scattering. There is no large difference among the observed charged particle spectra from p + W, O + W, and S + W. We observe no sharp rise in $\langle p_t \rangle$ vs.E_t, but it must be noted that the detected p_t spectrum is affected by the hadronization process and reflects conditions at the time of freezeout of hadrons. Also, an increase in the cross section for large pt is expected from hard scattering of partons and does not necessarily indicate more exotic processes.

REFERENCES

1. See for example, Proc. of the Quark Matter Conferences in Brookhaven (1984), Helsinki (1984) and Asilomar (1986)
2. T. Akesson, et al., Z. Phys. C38, 383 (1988).
3. G. Baym, P. Braun-Munzinger and V. Ruuskanen, Phys.Lett. 190B, 29 (1987); A.D. Jackson and H. Boggild, Nucl. Phys. A470, 669 (1987).
4. A. Capella and J. Tran Thanh Van, Phys. Lett. 93B, 146 (1980).
5. B. Alper, et al., Nucl. Phys. B100, 237 (1975);
6. D. Antreasyan, et al., Phys. Rev. D19, 764 (1979).
7. H. Stroebele, et al., Z. Phys. C38, (1988).
8. D.A. Garbutt, et al., Phys. Lett. 67B, 355 (1977).
9. L. Van Hove, Phys. Lett. 118B, 138 (1982).
10. M. Kataja, P.V. Ruuskanen, L. McLerran and H. von Gersdorff, Phys. Rev. D34, 2755 (1986); X. Wang and R. Hwa, Phys. Rev. D35, 3409 (1987).